



HAL
open science

Influence of metallic vapours on thermodynamic and transport properties of two-temperature air plasma

Linlin Zhong, Xiaohua Wang, Yann Cressault, Philippe Teulet, Mingzhe Rong

► **To cite this version:**

Linlin Zhong, Xiaohua Wang, Yann Cressault, Philippe Teulet, Mingzhe Rong. Influence of metallic vapours on thermodynamic and transport properties of two-temperature air plasma. *Physics of Plasmas*, 2016, 23 (9), pp.093514. 10.1063/1.4963245 . hal-03418990

HAL Id: hal-03418990

<https://ut3-toulouseinp.hal.science/hal-03418990>

Submitted on 6 May 2022

HAL is a multi-disciplinary open access archive for the deposit and dissemination of scientific research documents, whether they are published or not. The documents may come from teaching and research institutions in France or abroad, or from public or private research centers.

L'archive ouverte pluridisciplinaire **HAL**, est destinée au dépôt et à la diffusion de documents scientifiques de niveau recherche, publiés ou non, émanant des établissements d'enseignement et de recherche français ou étrangers, des laboratoires publics ou privés.



Distributed under a Creative Commons Attribution - NonCommercial 4.0 International License

Influence of metallic vapours on thermodynamic and transport properties of two-temperature air plasma

Linlin Zhong,^{1,2} Xiaohua Wang,^{1,a)} Yann Cressault,² Philippe Teulet,² and Mingzhe Rong^{1,b)}

¹State Key Laboratory of Electrical Insulation and Power Equipment, School of Electrical Engineering, Xi'an Jiaotong University, Xi'an 710049, People's Republic of China

²LAPLACE (Laboratoire Plasma et Conversion d'Énergie), Université de Toulouse; CNRS, UPS, INPT; 118 route de Narbonne, F-31062 Toulouse, France

(Received 13 July 2016; accepted 8 September 2016; published online 27 September 2016)

The metallic vapours (i.e., copper, iron, and silver in this paper) resulting from walls and/or electrode surfaces can significantly affect the characteristics of air plasma. Different from the previous works assuming local thermodynamic equilibrium, this paper investigates the influence of metallic vapours on two-temperature (2 T) air plasma. The 2 T compositions of air contaminated by Cu, Fe, and Ag are first determined based on Saha's and Guldberg–Waage's laws. The thermodynamic properties (including mass density, specific enthalpy, and specific heat) are then calculated according to their definitions. After determining the collision integrals for each pair of species in air-metal mixtures using the newly published methods and source data, the transport coefficients (including electrical conductivity, viscosity, and thermal conductivity) are calculated for air-Cu, air-Fe, and air-Ag plasmas with different non-equilibrium degree θ (T_e/T_h). The influences of metallic contamination as well as non-equilibrium degree are discussed. It is found that copper, iron, and silver exist mainly in the form of Cu_2 , FeO , and AgO at low temperatures. Generally, the metallic vapours increase mass density at most temperatures, reduce the specific enthalpy and specific heat in the whole temperature range, and affect the transport properties remarkably from 5000 K to 20 000 K. The effect arising from the type of metals is little except for silver at certain temperatures. Besides, the departure from thermal equilibrium results in the delay of dissociation and ionization reactions, leading to the shift of thermodynamic and transport properties towards a higher temperature. *Published by AIP Publishing.* [<http://dx.doi.org/10.1063/1.4963245>]

I. INTRODUCTION

Air plasma is widely applied in circuit breakers, arc heaters, torches, and arc welding apparatus. In such arc devices, the metallic vapours (e.g., copper, iron, silver, etc.) resulting from walls and/or electrode surfaces can mix with air and thus affect arc characteristics.¹ To understand the patterns of air plasma more deeply and better, the presence of metallic impurities must be taken into account in the more and more sophisticated plasma modelling which requires more and more accurate basic properties, such as compositions, thermodynamic properties, transport coefficients, and radiation properties.

The investigation of the properties of air plasma could be traced back to 1963 when Yos² published the transport coefficients as well as radiated power of air plasma in a wide range of temperature and pressure. In 1978, Devoto *et al.*³ performed a measurement in a wall-stabilized air arc and deduced the electrical and thermal conductivity. In 1989, Bacri and Raffanel⁴ presented their calculated results for electrical conductivity, viscosity, and thermal conductivity of air plasma. After that in 1995, Murphy⁵ determined the transport properties including combined diffusion coefficients of air plasma mixed with argon, nitrogen, and oxygen. In 2000,

Capitelli *et al.*⁶ reported the lasted collision integrals for air species up to 100 000 K and then applied these data to calculate the transport coefficients of high-temperature air.⁷ Later in 2008, D'Angola *et al.*⁸ proposed a new approach to determine the equilibrium compositions in air plasma and improved the thermodynamic and transport properties. Recently, Cressault *et al.*^{9–11} paid attention to the influence of metallic vapours and calculated the thermodynamic, transport, diffusion, and radiation coefficients of air plasma contaminated by copper, iron, silver, and aluminum. Teulet *et al.*^{12,13} also studied the effects of copper on the properties and interruption ability of air arc in low-voltage circuit breakers.

It is noticeable that all the above previous works were conducted under the assumption of local thermodynamic equilibrium (LTE) which means that the temperature of electrons (T_e) is equal to that of heavy particles (T_h). However, the departure from thermal equilibrium arises when large temperature gradient exists (e.g., near the cold walls) and when electron concentration is not high enough to allow sufficient transfer of energy between electrons and heavy particles,^{14,15} which results in the different values of T_e and T_h . To solve the problems where LTE is not valid, Devoto¹⁶ derived the transport coefficients of a two-temperature (2 T) plasma assuming a complete decoupling between electrons and heavy particles. Rat *et al.*^{17,18} took the coupling into account and developed an improved 2 T theory which can be applied in the calculation of combined diffusion coefficients.

^{a)}xhw@mail.xjtu.edu.cn

^{b)}mzrong@mail.xjtu.edu.cn

Concerning the 2T air plasma, few works could be found except for the work by Ghorui *et al.*¹⁹ who studied the 2T properties of N₂-O₂ mixtures which are the main components of air. However, the metallic impurities were not considered in their calculation, which is the focus in the present work.

In this paper, the influences of metallic vapours (copper, iron, and silver) on the compositions, thermodynamic properties (mass density, specific enthalpy, and specific heat), and transport coefficients (electrical conductivity, viscosity, and thermal conductivity) are investigated in the 2T air plasma with different non-equilibrium degree T_e/T_h (denoted as θ) at temperatures up to 40 000 K. To avoid considering the condensed species (e.g., metals and their oxides at low temperatures), the lower limit of temperature in this work is set to be 2000 K, following the recommendation of Cressault *et al.*^{9,11} The pressure is fixed at 1 bar and all the mixing ratios are given in molar proportion. The rest Sections II–V are dedicated, respectively, to 2T compositions, thermodynamic properties, collision integrals, and transport coefficients.

II. COMPOSITIONS OF 2T PLASMA

A. Calculation method

Compositions of plasma are one of the prerequisites for the calculation of both thermodynamic and transport properties. The equilibrium compositions in LTE are usually determined by minimization of the Gibbs free energy^{20,21} which is not necessary to define the free and bound species as another method (Saha's and Guldberg–Waage's laws) requires.²² However, for a 2T plasma, a set of nonlinear equations based on dissociation (Guldberg–Waage's law) and ionization (Saha's law) reactions have to be established in calculating 2T compositions. Potapov²³ and van de Sanden *et al.*²⁴ deduced, respectively, two different forms of equation for ionization reactions in 2T plasmas. In this work, the latter method is used as formulated in (1) and (2), which was recommended by Gleizes *et al.*²⁵ and also adopted in Refs. 15, 19, and 26

$$\frac{n_a n_b}{n_c} = \frac{Q_a^{\text{int}} Q_b^{\text{int}}}{Q_c^{\text{int}}} \left(\frac{2\pi k T_h}{h^2} \right)^{3/2} \left(\frac{m_a m_b}{m_c} \right)^{3/2} \exp\left(-\frac{E_d}{k T_{ex}}\right), \quad (1)$$

$$\frac{n_e n_{a^{(z+1)+}}}{n_{a^{z+}}} = 2 \frac{Q_{a^{(z+1)+}}^{\text{int}}}{Q_{a^{z+}}^{\text{int}}} \left(\frac{2\pi m_e k T_e}{h^2} \right)^{3/2} \exp\left(-\frac{E_i - \Delta E_i}{k T_{ex}}\right), \quad (2)$$

where m_i , n_i , and Q_i^{int} are the mass, number density, and internal partition function of species i , respectively. In the calculation of Q_i^{int} , T_e is used for the electronic part and T_h for vibrational and rotational parts. k is the Boltzmann constant and h is the Planck constant. E_d is the dissociation energy of the reaction $c \leftrightarrow a + b$. E_i is the ionization energy of species a^{z+} and ΔE_i is the corresponding ionization energy lowering. T_{ex} is the excitation temperature. In this work, T_h is set as T_{ex} for dissociation reactions and ionization of molecules, and for atomic ionization, T_e is used as the excitation temperature.

Equations (1) and (2) for the reactions given in Table I, together with chemical equilibrium, electrical neutrality, and

Dalton's law can be solved to obtain 2T compositions. Besides, the pressure correction due to Debye–Hückel effect^{20,25} is also taken into account in the present work. The basic data for the calculation of internal partition functions were compiled from NIST database²⁷ and the NIST-JANAF Thermochemical Tables.²⁸ The lowering of ionization energy is considered in the calculation of atomic partition functions, and an iterative procedure is therefore applied until the convergence of compositions.

B. Results and discussion

The air composed of 78% N₂, 21% O₂, and 1% Ar by volume is used in this work. As illustrated in Table I, 44 species involved in 10 dissociation and 28 ionization elementary reactions are taken into account.

Figures 1(a) and 1(b) show the compositions of pure air plasma with θ (T_e/T_h) = 1 and 3, respectively, as a function of electron temperature T_e up to 40 000 K at ambient pressure, and Figures 2–4 show the 2T compositions of 90%air–10%Cu, 90%air–10%Fe, and 90%air–10%Ag plasmas, respectively, with $\theta = 3$. In LTE air plasma ($\theta = 1$), the ionization of NO contributes to the early increase of electrons, whereas in non-LTE condition ($\theta = 3$), atomic oxygen replaces NO to generate electrons through ionization because of the delay of reactions resulting from the inequality of T_e and T_h . In addition, due to the lower ionization potential (N 14.53 eV, O 13.62 eV, Ar 15.76 eV, Cu 7.73 eV, Fe 7.90 eV, and Ag 7.58 eV (Ref. 27)) than nitrogen, oxygen, and argon atoms, Cu, Fe, and Ag cause the mixtures to ionize at lower temperatures. Compared with air-Cu mixture in which copper exists mainly in the form of its dimer (Cu₂) at low temperatures, metal oxides (FeO and AgO) instead of metal dimers (Fe₂ and Ag₂) dominate the air-Fe and air-Ag mixtures together with N₂ and O₂ in the low temperature range. This is consistent with the result by Cressault *et al.*⁹ for air-Fe plasma in LTE. Moreover, although Ag has the lowest ionization potential among the three metals, Ag⁺ starts to affect the mixture at a higher temperature than Cu⁺ and Fe⁺. This is because AgO is more difficult to decompose and generate Ag than Cu₂ and FeO to generate Cu and Fe, considering that the dissociation energy of Cu₂, FeO, and AgO are 1.97 eV, 4.29 eV, and 4.58 eV, respectively.

TABLE I. Elementary chemical reactions in Air-Cu, Air-Fe, and Air-Ag plasmas.

Dissociation	Ionization	Ionization	Ionization
N ₂ ↔ N + N	N ₂ ↔ N ₂ ⁺ + e [−]	O ↔ O ⁺ + e [−]	Fe ↔ Fe ⁺ + e [−]
O ₂ ↔ O + O	O ₂ ↔ O ₂ ⁺ + e [−]	O ⁺ ↔ O ²⁺ + e [−]	Fe ⁺ ↔ Fe ²⁺ + e [−]
NO ↔ N + O	NO ↔ NO ⁺ + e [−]	O ²⁺ ↔ O ³⁺ + e [−]	Fe ²⁺ ↔ Fe ³⁺ + e [−]
NO ₂ ↔ NO + O	N ₂ [−] ↔ N ₂ + e [−]	Ar ↔ Ar ⁺ + e [−]	Fe [−] ↔ Fe + e [−]
Cu ₂ ↔ Cu + Cu	O ₂ [−] ↔ O ₂ + e [−]	Ar ⁺ ↔ Ar ²⁺ + e [−]	Ag ↔ Ag ⁺ + e [−]
CuO ↔ Cu + O	NO ₂ [−] ↔ NO ₂ + e [−]	Ar ²⁺ ↔ Ar ³⁺ + e [−]	Ag ⁺ ↔ Ag ²⁺ + e [−]
Fe ₂ ↔ Fe + Fe	N ↔ N ⁺ + e [−]	Cu ↔ Cu ⁺ + e [−]	Ag ²⁺ ↔ Ag ³⁺ + e [−]
FeO ↔ Fe + O	N ⁺ ↔ N ²⁺ + e [−]	Cu ⁺ ↔ Cu ²⁺ + e [−]	Ag [−] ↔ Ag + e [−]
Ag ₂ ↔ Ag + Ag	N ²⁺ ↔ N ³⁺ + e [−]	Cu ²⁺ ↔ Cu ³⁺ + e [−]	
AgO ↔ Ag + O	O [−] ↔ O + e [−]	Cu [−] ↔ Cu + e [−]	

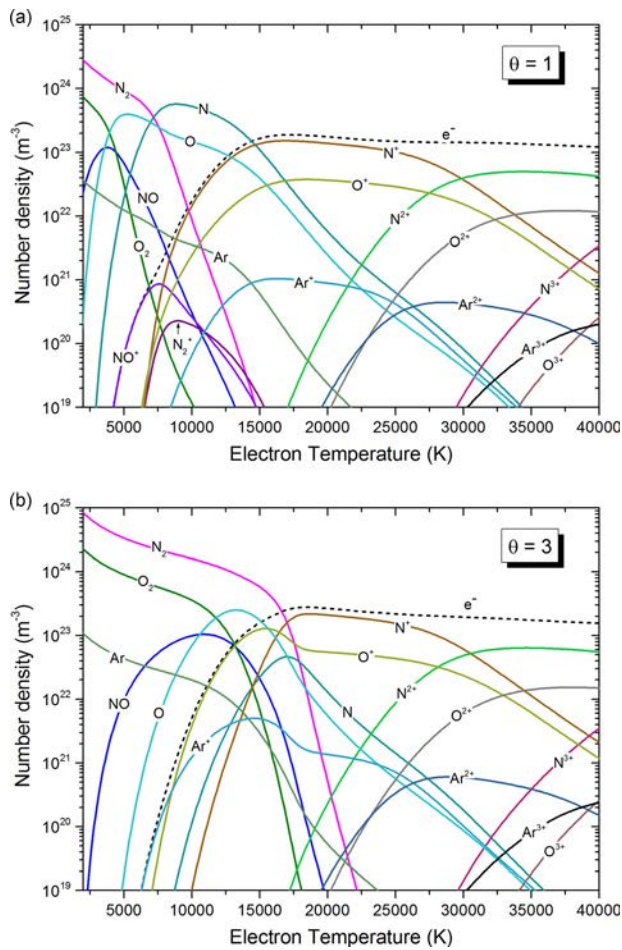


FIG. 1. Compositions of pure air plasma as a function of T_e at 1 bar with (a) $\theta = 1$ and (b) $\theta = 3$.

III. THERMODYNAMIC PROPERTIES OF 2T PLASMA

A. Calculation method

Based on the compositions and internal partition functions, the thermodynamic properties can be calculated straightforwardly according to their definitions. The mass

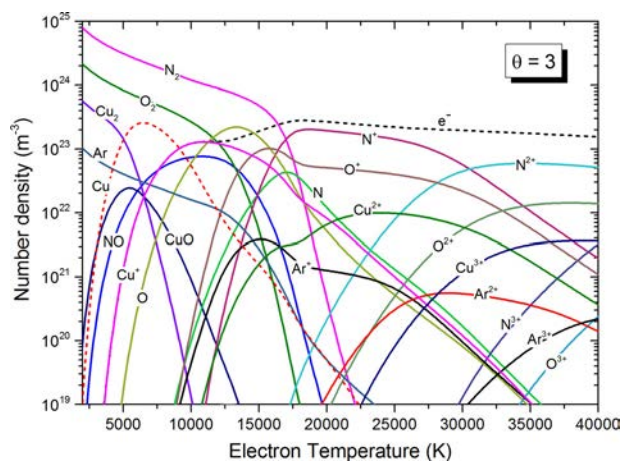


FIG. 2. 2T composition of air plasma contaminated by 10% Cu (molar proportion) as a function of T_e with $\theta = 3$ at 1 bar.

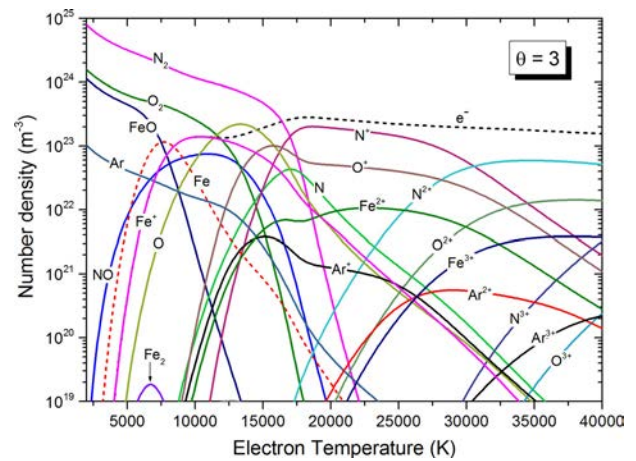


FIG. 3. 2T composition of air plasma contaminated by 10% Fe (molar proportion) as a function of T_e with $\theta = 3$ at 1 bar.

density of a 2T plasma is the sum of product of mass and number density for each species, which is the same as that in a LTE plasma.²⁰ For specific enthalpy of each species, the three components (translational, reaction, and internal parts) should be taken into account as described in Ref. 14. In the calculation of the derivative of partition functions with respect to temperature, it is assumed that the electronic partition functions Q_i^{el} are governed by electron temperature T_e , and the vibrational partition functions Q_i^{vib} and rotational partition functions Q_i^{rot} are governed by heavy particle temperature T_h . Therefore, the specific enthalpies are calculated as follows:¹⁴

For electrons

$$h_e = \frac{5k}{2\rho} n_e T_e. \quad (3)$$

For monoatomic species

$$h_i = \frac{5k}{2\rho} n_i T_i + \frac{1}{\rho} n_i E_i + \frac{k}{\rho} n_i \left(T_e^2 \frac{\partial \ln Q_i^{el}}{\partial T_e} \right). \quad (4)$$

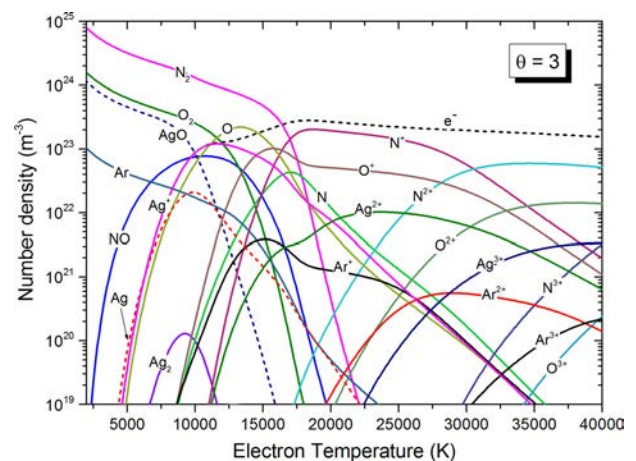


FIG. 4. 2T composition of air plasma contaminated by 10% Ag (molar proportion) as a function of T_e with $\theta = 3$ at 1 bar.

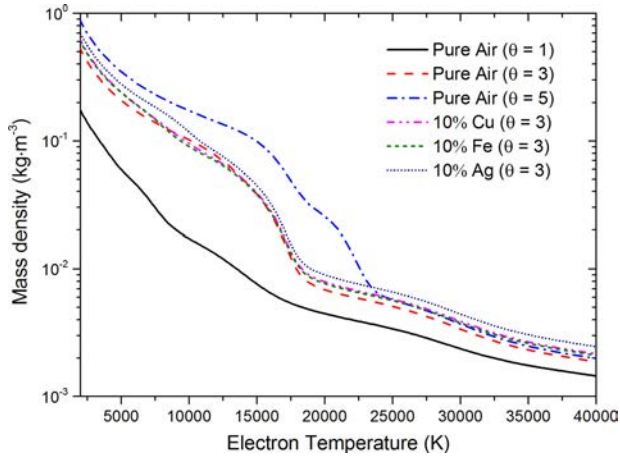


FIG. 5. Mass density of air and air-metal plasmas as a function of electron temperature with different non-equilibrium degree θ at 1 bar.

For molecular species

$$h_i = \frac{5k}{2\rho} n_i T_i + \frac{1}{\rho} n_i E_i + \frac{k}{\rho} n_i \left(T_e^2 \frac{\partial \ln Q_i^{el}}{\partial T_e} + T_h^2 \frac{\partial \ln(Q_i^{vib} Q_i^{rot})}{\partial T_h} \right), \quad (5)$$

where ρ is the mass density and E_i is the formation energy.

Concerning specific heat (at constant pressure), Colombo *et al.*^{15,26} interpreted the derivative of total specific enthalpy with respect to T_e as the total specific heat. However, in order to perform a numerical simulation of a two-temperature plasma, it is necessary to separate the electron specific heat C_{pe} and heavy particle specific heat C_{ph} from the total one. Therefore, in this work, C_{pe} is calculated as the derivative of specific enthalpy of electrons with respect to T_e , and C_{ph} is determined as the derivative of specific enthalpy of heavy particles with respect to T_h . The same calculation procedure was adopted by Ghorui *et al.*¹⁹

B. Results and discussion

Figure 5 shows the mass density of pure air and air mixtures contaminated by 10% Cu, Fe, and Ag. A sharp drop is observed for each curve in the temperature range in which the decompositions of molecules occur. With the increase of non-equilibrium degree θ , this sharp decrease is shifted to a higher temperature because the dissociations are delayed. Additionally, it can be seen that metallic vapours raise the value of mass density at most temperatures. And due to the larger mass (Cu 63.5 g mol⁻¹, Fe 55.8 g mol⁻¹, and Ag 107.9 g mol⁻¹), silver contamination affects the mass density more strongly than copper and iron.

The specific enthalpy of air and air-metal plasmas is described in Figure 6. It is found that the specific enthalpy is strongly sensitive to non-equilibrium degree θ at relatively low temperatures, whereas it becomes less sensitive to θ at higher temperatures. This can be attributed to the delay of the reactions resulting from the difference between T_h and T_e , considering that T_h is used as excitation temperature for dissociation and ionization of molecular species while T_e is used in

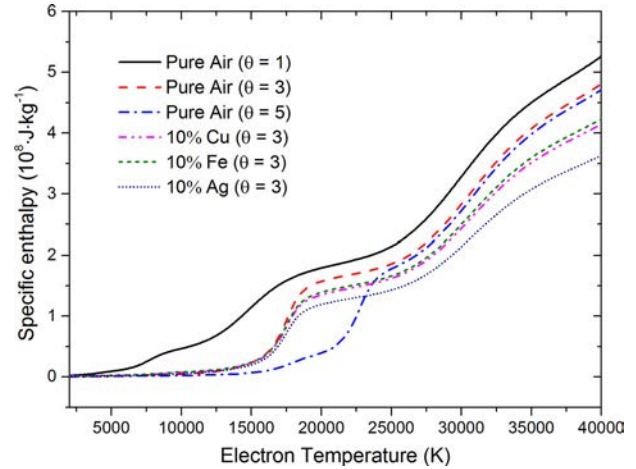


FIG. 6. Specific enthalpy of air and air-metal plasmas as a function of electron temperature with different non-equilibrium degree θ at 1 bar.

atomic ionization. It is also observed that the contamination of metallic vapours generally reduces the specific enthalpy of mixtures, because the enthalpies of metals are smaller than those of air species. Among the three mixtures, the specific enthalpy of air-Cu plasma is close to that of air-Fe but much larger than that of air-Ag, especially at high temperatures.

Figures 7 and 8 show the electron specific heat C_{pe} and heavy particle specific heat C_{ph} for pure air and air-metal mixtures at temperatures up to 40000 K. As discussed by Ghorui *et al.*,¹⁹ the peaks of C_{pe} correspond to the ionization reactions, and the peaks of C_{ph} result from both ionization and dissociation reactions. For example, in Figure 7, two peaks are observed in a LTE air plasma. The first peak corresponds to the first ionization of atomic N and O, and the second peak corresponds to the second ionization of atomic N. When the non-equilibrium degree θ increases, the dissociation of N₂ and O₂ is delayed, leading to the shift of peaks, considering that the ionization of atoms occurs only after the dissociation of their parental molecules. It is interesting that three peaks can be observed when $\theta = 5$. This is because the ionization energy of atomic N and O are close to each other but the dissociation energy of N₂ and O₂ are much different. As a result, the first peak in this case arises from the first

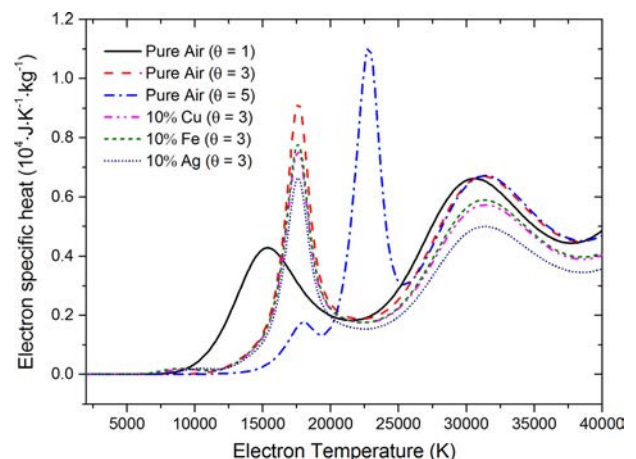


FIG. 7. Electron specific heat C_{pe} of air and air-metal plasmas as a function of electron temperature with different non-equilibrium degree θ at 1 bar.

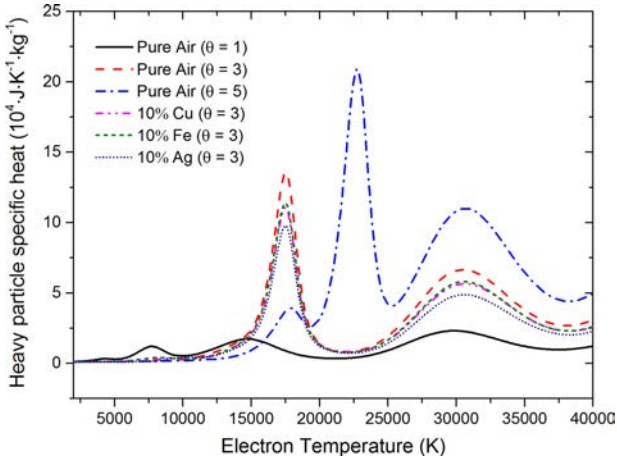


FIG. 8. Heavy particle specific heat C_{ph} of air and air-metal plasmas as a function of electron temperature with different non-equilibrium degree θ at 1 bar.

ionization of atomic O, and the other two peaks correspond to the first and second ionizations of atomic N, respectively. For air-metal mixtures, the contamination of metallic vapours leads to the decrease of C_{pe} and C_{ph} because of the decline of the molecular decompositions and the reinforcement of the metallic ionization. Moreover, as discussed for specific enthalpy, copper and iron vapours present the similar influence on both C_{pe} and C_{ph} , and silver vapour shows larger influence, i.e., reducing C_{pe} and C_{ph} more significantly, especially at high temperatures.

IV. COLLISION INTEGRALS

The calculation of the transport coefficients was developed based on the Chapman–Enskog method which requires the knowledge of collision integrals.^{29,30} The reduced collision integral characterized by the order (l,s) between two particles i and j is defined as follows:^{19,29,31}

$$\bar{\Omega}_{ij}^{(l,s)} = \frac{4(l+1)}{\pi(s+1)! [2l+1 - (-1)^l]} \int_0^\infty e^{-\gamma_{ij}^2} \gamma_{ij}^{2s+3} Q_{ij}^{(l)}(\gamma_{ij}) d\gamma_{ij}, \quad (6)$$

where $\gamma_{ij} = (\varepsilon/kT_{ij}^*)^{1/2}$, and ε is the kinetic energy. It is notable that the unified temperature T in LTE is replaced by the effective one T^* ij in a 2T model

$$T_{ij}^* = \frac{m_i T_j + m_j T_i}{m_i + m_j}, \quad (7)$$

where T_i and T_j are temperature of the particles i and j , respectively.

In order to calculate the collision integrals, four kinds of interactions, namely, neutral-neutral, neutral-ion, neutral-electron, and charged-charged, should be considered. For charged-charged interactions, the Coulomb potential is used as described in our previous work²⁹ without consideration of ions in the calculation of Debye length. For neutral-electron interactions, the collision integrals for air species, Cu, Fe, and Ag were compiled from the work by Capitelli *et al.*,⁶ Wang *et al.*,²⁹ Cressault *et al.*,⁹ and André *et al.*,³² respectively. For

the collisions between electrons and NO_2 , metal dimers (Cu_2 , Fe_2 , and Ag_2), and metal oxides (CuO , FeO , and AgO), the polarizability potential is used to calculate the collision integrals. For neutral-neutral and neutral-ion interactions, the Lennard–Jones like phenomenological model potential^{33,34} is adopted instead of the classical potential for the reason presented in our previous work.^{29,30} Furthermore, the resonant charge-exchange process, which plays an important role in determining collision integrals between a neutral particle and its ion when the order l is even,²⁹ is also taken into account using an empirical mixing rule proposed by Murphy.^{5,35,36} The fitting parameters (A and B) of charge-exchange cross sections were compiled from Refs. 6, 32, 37, and 38.

To determine the transport coefficients in a given approximation order, nine kinds of collision integrals $\bar{\Omega}(1,1)$, $\bar{\Omega}(1,2)$, $\bar{\Omega}(1,3)$, $\bar{\Omega}(1,4)$, $\bar{\Omega}(1,5)$, $\bar{\Omega}(2,2)$, $\bar{\Omega}(2,3)$, $\bar{\Omega}(2,4)$, and $\bar{\Omega}(3,3)$ are calculated in this work. The values of $\bar{\Omega}(1,1)$ for N_2 - N_2 , O_2 - O_2 , N-N, O-O, Cu-Cu, Fe-Fe, and Ag-Ag interactions are displayed in Figure 9, indicating that the collision integrals of metals are much larger than those of air species. Moreover, among the three metals, Fe-Fe and Cu-Cu pairs present the largest and smallest collision integrals, respectively. These differences can help to understand the influence of metallic vapours on the transport coefficients of air plasma discussed in Section V.

V. TRANSPORT COEFFICIENTS OF 2T PLASMA

A. Calculation method and its validation

The transport coefficients (including electrical conductivity, viscosity, and thermal conductivity in this paper) are usually calculated based on the Chapman–Enskog method.^{29,30} As stated in the section of Introduction, Devoto¹⁶ and Rat *et al.*^{17,18} deduced two sets of formulas for transport properties in 2T plasmas. The difference between the two methods lies in the treatment of coupling between electrons and heavy particles. It has been demonstrated by Colombo *et al.*²⁶ that this coupling shows little influence on transport coefficients. Therefore, for electrical conductivity, the expression in the third order approximation reported by Devoto¹⁶ is used in this

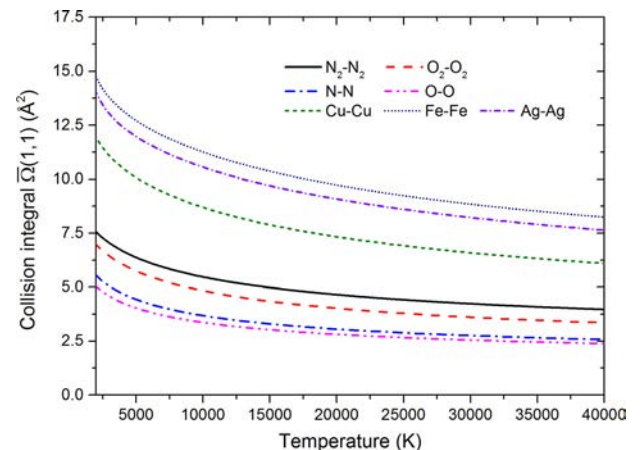


FIG. 9. Collision integrals $\bar{\Omega}(1,1)$ for N_2 - N_2 , O_2 - O_2 , N-N, O-O, Cu-Cu, Fe-Fe, and Ag-Ag interactions using the Lennard–Jones like phenomenological potential.

work, neglecting the contribution of ions. For viscosity, the approximate formula presented by Bonnefoi³⁹ is adopted, which was also used by Colombo *et al.*¹⁵ and Ghorui *et al.*¹⁹ The calculation of thermal conductivity is more complicated as the total thermal conductivity is represented as the sum of three components, the translational thermal conductivity, internal thermal conductivity, and reaction thermal conductivity, respectively.^{29,40} Furthermore, since electrons and heavy particles have different temperatures in 2T plasmas, the thermal conductivity can be separated for them as electron thermal conductivity κ_e and heavy particle thermal conductivity κ_h , respectively¹⁹

$$\kappa_e = \kappa_e^{tr} + \kappa_e^{react}, \quad (8)$$

$$\kappa_h = \kappa_h^{tr} + \kappa_h^{int} + \kappa_h^{react}, \quad (9)$$

where κ_e^{tr} and κ_h^{tr} are translational components, κ_e^{react} and κ_h^{react} are reactive components, and κ_h^{int} is internal component for heavy particles.

For the calculation of translation thermal conductivity, the expressions deduced by Devoto^{16,19,29} are used. For the internal thermal conductivity, the second order Eucken approximation^{19,29} is applied. For reaction thermal conductivity, Chen and Li⁴¹ developed a method to calculate K_e^{react} and K_h^{react} separately for argon plasma, using the basic concept of Butler and Brokaw⁴² who derived a formula for reaction thermal conductivity of plasmas in LTE. Ghorui *et al.*¹⁹ applied the same method in more complex mixtures, which is adopted in this work. Assuming R independent reactions generating N species in a plasma, the two components of reaction thermal conductivity can be expressed as¹⁹

$$\kappa_e^{react} = \sum_{r=1}^R \Delta h_r \frac{n}{\rho k T_h} \sum_{j=1}^N \frac{T_h}{T_j} m_j D_{rj}^a \frac{\partial p_j}{\partial T_e}, \quad (10)$$

$$\kappa_h^{react} = \sum_{r=1}^R \Delta h_r \frac{n}{\rho k T_h} \sum_{j=1}^N \frac{T_h}{T_j} m_j D_{rj}^a \frac{\partial p_j}{\partial T_h}, \quad (11)$$

where p_j is the partial pressure of species j , n and ρ are total number density and mass density, respectively, Δh_r is the enthalpy of reaction r , and D_{rj}^a is the ambipolar diffusion coefficient. The total reaction thermal conductivity κ_{tot}^{react} can thus be represented by (9) with respect to the gradient of heavy particle temperature⁴¹

$$\kappa_{tot}^{react} = \kappa_h^{react} + \theta \cdot \kappa_e^{react}. \quad (12)$$

In order to validate the calculation described above, the electrical conductivity, viscosity, and heavy particle translational thermal conductivity were calculated for Ar, N₂, and O₂ plasmas, respectively, in comparison with the results published by Rat *et al.*,⁴³ Colombo *et al.*,⁴⁴ Murphy,⁵ and Murphy and Arundelli.⁴⁰ All the calculations were performed at ambient pressure. As shown in Figures 10–12, respectively, a good agreement is obtained, and the slight differences observed in peaks are due mainly to the collision integrals which were calculated using different potential or compiled from different sources.

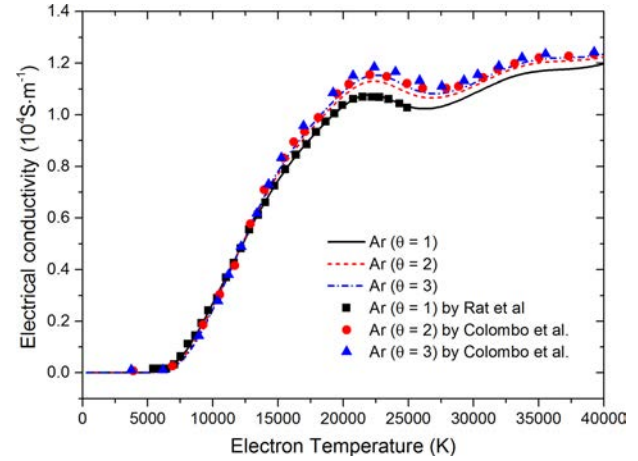


FIG. 10. Electrical conductivity of argon plasma as a function of electron temperature with different non-equilibrium degree θ at 1 bar, compared with the works by Rat *et al.*⁴³ and Colombo *et al.*⁴⁴

B. Electrical conductivity

Based on the above method, electrical conductivity of 2T air plasma contaminated by copper, iron, and silver vapor are calculated and discussed in this subsection. Figure 13 illustrates the electrical conductivity of pure air up to 40 000 K at 1 bar with three different values of θ (1, 3, and 5). The result in LTE ($\theta = 1$) agrees exactly with the works by Murphy⁵ and D'Angola *et al.*⁸ As can be seen, due to the delay of dissociation and ionization reactions, the electrical conductivity is shifted to a higher electron temperature as θ increases. Additionally, in a plasma with a higher value of θ , also because of the delay of decomposition of molecules, the atoms generated from the decomposition reactions start to ionize at a higher temperature and thus ionize more easily, leading to a more rapid increase of electrical conductivity.

The influence of metallic vapours on electrical conductivity of air plasma is described in Figure 14 with $\theta = 3$. Owing to their low ionization potential, Cu, Fe, and Ag raise the electrical conductivity of air-metal mixtures significantly between

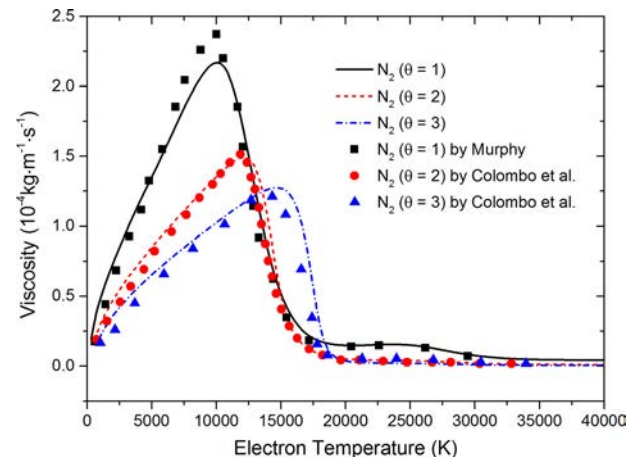


FIG. 11. Viscosity of N₂ plasma as a function of electron temperature with different non-equilibrium degree θ at 1 bar, compared with the works by Murphy⁵ and Colombo *et al.*⁴⁴

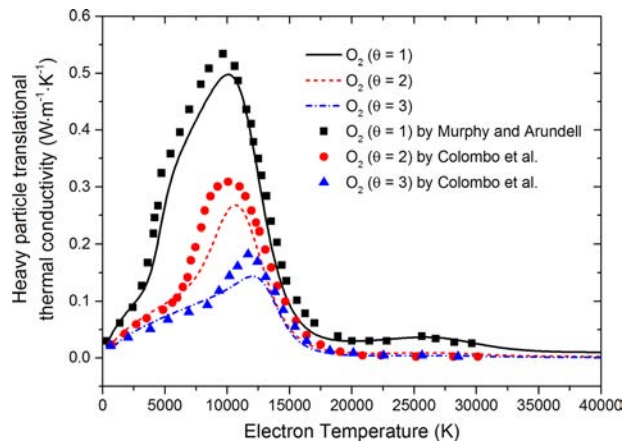


FIG. 12. Heavy particle translational thermal conductivity of O_2 plasma as a function of electron temperature with different non-equilibrium degree θ at 1 bar, compared with the works by Murphy and Arundelli⁴⁰ and Colombo *et al.*⁴⁴

5000 K and 17 000 K. However, at higher temperatures, the ionization of nitrogen and oxygen starts to dominate the reactions in the mixtures as shown in Figures 2–4, weakening the effect of metals and diminishing the difference between different metals which can be observed obviously at 5000–17 000 K.

C. Viscosity

Viscosity representing the transport of momentum due to a gradient in the velocity is one of the essential parameters in plasma modellings.²⁹ Figure 15 compares the present results of pure air with the results in LTE published by Murphy⁵ and Capitelli *et al.*⁷ A good agreement can be observed except for the distinction around the peak. As discussed in our previous work,²⁹ this discrepancy is due mainly to the different values of collision integrals for neutral-neutral interactions which are responsible for the peaks of viscosity in the medium temperature range. The influence of non-equilibrium degree is also displayed in Figure 15, showing that the departure from thermal equilibrium shifts the viscosity towards a higher

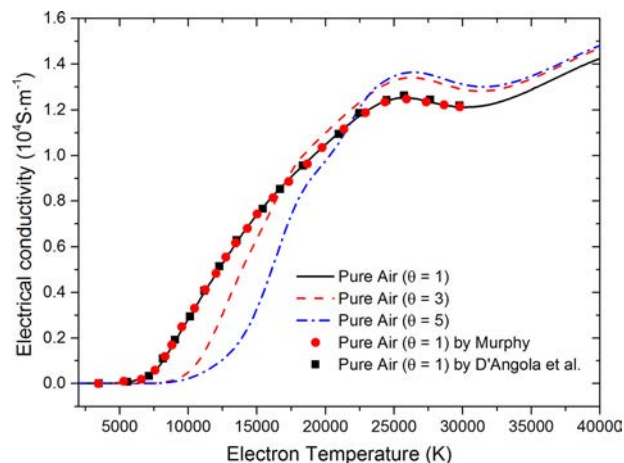


FIG. 13. Electrical conductivity of air plasma as a function of electron temperature with different non-equilibrium degree θ at 1 bar, compared with the works in LTE ($\theta = 1$) by Murphy⁵ and D'Angola *et al.*⁸

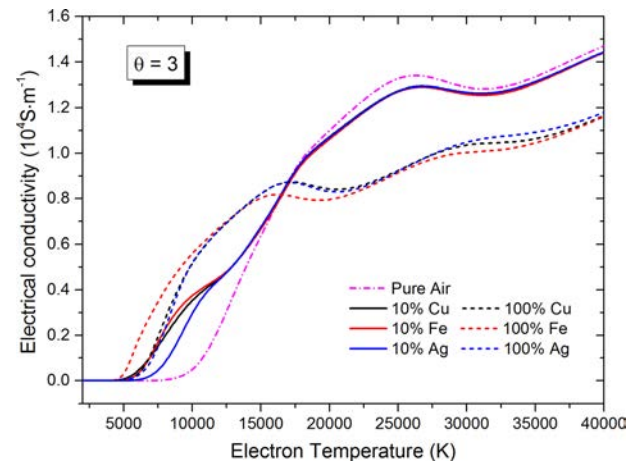


FIG. 14. Electrical conductivity of pure air, pure metal (Cu, Fe, Ag), and air-metal mixture as a function of electron temperature with $\theta = 3$ at 1 bar.

temperature and reduces the maximum. This can be explained by the delay of dissociation reactions, considering that the interactions between neutral particles dominate the peak of the viscosity.

Figure 16 highlights the effect of metallic vapours on the viscosity of air plasma with $\theta = 3$ at ambient pressure. Generally, considering that viscosity is in inverse proportion to collision integrals,²⁹ the presence of metals decreases the viscosity at 5000–17 000 K because neutral particles including atoms rule the mixtures in this temperature range and the metals (Cu-Cu, Fe-Fe, Ag-Ag) have the largest collision integrals among them (as shown in Figure 9). However, at higher temperatures, ions and the corresponding Coulomb potential take the dominant place of neutral species and the neutral-neutral potential, diminishing the influence of metals, because the Coulomb potential depends not on the types of ions but on their charges. It is worthy to point out that silver influences the viscosity more dramatically before the viscosity reaches the peak. This can be attributed to the delay of dissociation of AgO compared with Cu_2 and FeO as discussed in Section II.

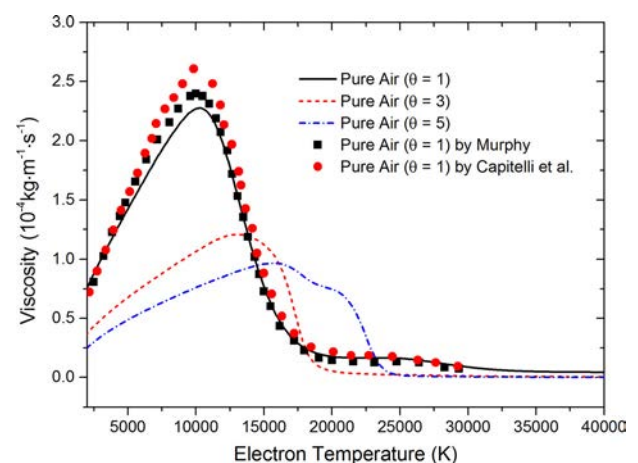


FIG. 15. Viscosity of air plasma as a function of electron temperature with different non-equilibrium degree θ at 1 bar, compared with the works in LTE ($\theta = 1$) by Murphy⁵ and Capitelli *et al.*⁷

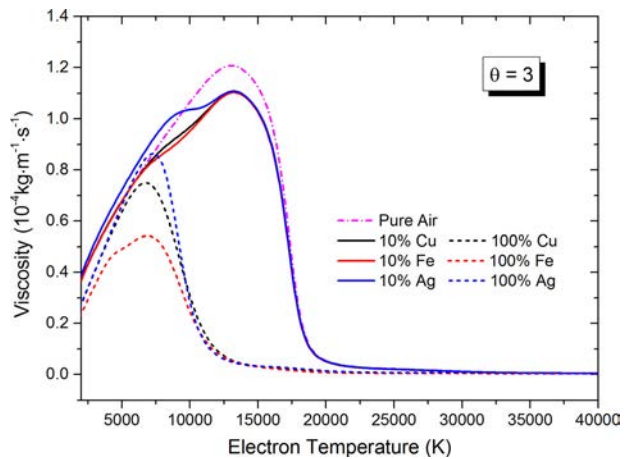


FIG. 16. Viscosity of pure air, pure metal (Cu, Fe, Ag), and air-metal mixture as a function of electron temperature with $\theta=3$ at 1 bar.

D. Thermal conductivity

Thermal conductivity is more complicated under 2T condition than in LTE because of different components both for electrons and heavy particles. Figure 17 compares the total reaction thermal conductivity of air plasma in LTE ($\theta=1$) with the results calculated by Murphy,⁵ and shows a good agreement. According to the previous works,^{5,9,29} the peaks of reaction thermal conductivity correspond to the predominate reactions in the corresponding temperature range. For example, the three peaks observed in pure air ($\theta=1$) are attributed to the dissociation of N_2 and O_2 and ionization of their constituent atoms. With the delay of the corresponding reactions, increasing θ inevitably leads to the shift of peaks. It is interesting that only one peak can be observed when $\theta=3$. To explain this, each component of the thermal conductivity in air plasma with $\theta=3$ is plotted in Figure 18. It can be observed that heavy particle translational thermal conductivity κ_h^{tr} , heavy particle reaction thermal conductivity κ_h^{reac} , and electron translational thermal conductivity κ_e^{tr} become the key components successively with the increase of temperature. Coincidentally, one of the peaks of electron reaction thermal conductivity κ_e^{reac} at around 17 000 K is

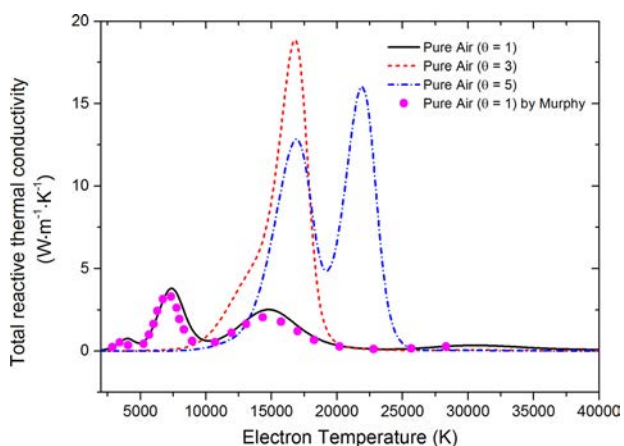


FIG. 17. Total reaction thermal conductivity of air plasma as a function of electron temperature with different non-equilibrium degree θ at 1 bar, compared with the work in LTE ($\theta=1$) by Murphy.⁵

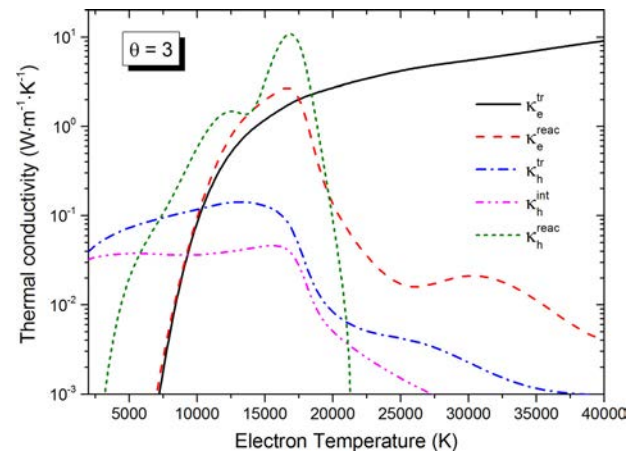


FIG. 18. Components of thermal conductivity of air plasma with $\theta=3$ as a function of electron temperature at 1 bar.

masked by the larger peak of κ_h^{reac} , leading to the disappearance of one of the peaks in total reaction thermal conductivity as observed in Figure 17.

The discussion of influence of metallic vapours on thermal conductivity is divided into two parts for electrons and heavy particles, respectively. Figures 19 and 20 describe the electron thermal conductivity κ_e and heavy particle thermal conductivity κ_h , respectively, in pure air, pure metals, and air-metal mixtures with $\theta=3$. Below 6000 K, κ_e is very small because of the weak ionization. From 6000 to 13 000 K, the metals with stronger ionization ability raise the values of κ_e . On the contrary, from 13 000 to 20 000 K, in which ionization of nitrogen and oxygen rules the reactions, the mixing of metals reduces the amount of nitrogen and oxygen, and thus decreases κ_e . Above 20 000 K, the complete ionization of atoms causes the electron translational thermal conductivity to be the key component, and therefore, the influence arising from metals diminishes. Compared with κ_e , the effect of metals on κ_h is clearer. At 8000–20 000 K, beyond which κ_h is negligible, the metal contamination reduces the value of κ_h , due to the decrease of the amounts of nitrogen and oxygen which dominate in this temperature

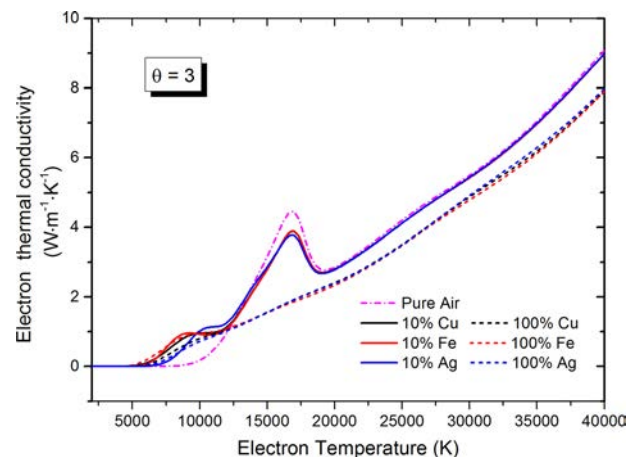


FIG. 19. Electron thermal conductivity of pure air, pure metal (Cu, Fe, Ag), and air-metal mixture as a function of electron temperature with $\theta=3$ at 1 bar.

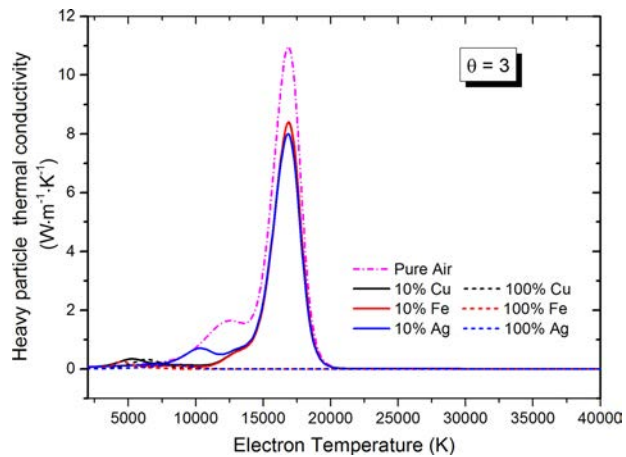


FIG. 20. Heavy particle thermal conductivity of pure air, pure metal (Cu, Fe, Ag), and air-metal mixture as a function of electron temperature with $\theta = 3$ at 1 bar.

range. Generally, the difference in metal type is little except for Ag in certain temperature range. As discussed above, this exception is the consequence of the higher dissociation energy of AgO than that of Cu₂ and FeO.

VI. CONCLUSIONS

This paper is devoted to the thermodynamic properties and transport coefficients of 2 T air plasma contaminated by copper, iron, and silver. The 2 T compositions of pure air, air-Cu, air-Fe, and air-Ag are first determined by solving the nonlinear equation system based on Saha's and Guldberg–Waage's laws. The specific enthalpy and specific heat are then calculated based on the compositions. Next, the collision integrals describing the interactions between each particle in the air-metal plasmas are determined. Lastly, the electrical conductivity, viscosity, and thermal conductivity are calculated. The influences of metallic vapours and non-equilibrium degree on air-metal plasmas are discussed. The conclusions are drawn as follows.

- (a) Copper, iron, and silver exist mainly in the form of Cu₂, FeO, and AgO at low temperatures, and AgO is more difficult to decompose than Cu₂ and FeO.
- (b) Generally, the contamination of metallic vapours increases the mass density and reduces the specific enthalpy and specific heat of air plasmas.
- (c) The ionization energy of atomic O and N is close to each other, and the dissociation energy of O₂ and N₂ is much different, which results in the different number of peaks in specific heat when non-equilibrium degree increases.
- (d) Collision integrals of Cu-Cu, Fe-Fe, and Ag-Ag are much larger than those of air species, which inevitably affect the transport properties of the plasma.
- (e) The departure from thermal equilibrium causes the delay of dissociation and ionization reactions, leading to the shift of thermodynamic properties and transport coefficients towards a higher temperature.
- (f) The contamination of metallic vapours affects the transport properties significantly from 5000 K to 20 000 K.

Beyond this range, the influence of metallic vapours is negligible.

- (g) The influence arising from the type of metals is little except for silver at certain temperatures.

ACKNOWLEDGMENTS

This work was supported by the National Key Basic Research Program (“973” Program) of China (No. 2015CB251001), the National Natural Science Foundation of China (Nos. 51407136 and 51521065), and the Fok Ying Tong Education Foundation (No. 141058). This work was also supported by the program of China Scholarship Council (CSC) for joint-Ph.D. students (No. 201506280131).

- ¹A. B. Murphy, *J. Phys. D: Appl. Phys.* **43**, 434001 (2010).
- ²J. M. Yos, “Transport properties of nitrogen, hydrogen, oxygen, and air to 30,000 K,” Technical Memorandum No. RAD-TM-63-7 (1963).
- ³R. S. Devoto, U. H. Bauder, J. Caillietau, and E. Shires, *Phys. Fluids* **21**, 552 (1978).
- ⁴J. Bacri and S. Raffanel, *Plasma Chem. Plasma Process.* **9**, 133–154 (1989).
- ⁵A. B. Murphy, *Plasma Chem. Plasma Process.* **15**, 279–308 (1995).
- ⁶M. Capitelli, C. Gorse, and S. Longo, *J. Thermophys. Heat Transfer* **14**, 259–268 (2000).
- ⁷M. Capitelli, G. Colonna, C. Gorse, and A. D’Angola, *Eur. Phys. J. D* **11**, 279–289 (2000).
- ⁸A. D’Angola, G. Cononna, C. Gorse, and M. Capitelli, *Eur. Phys. J. D* **46**, 129–150 (2008).
- ⁹Y. Cressault, R. Hannachi, Ph. Teulet, A. Gleizes, J.-P. Gonnet, and J.-Y. Battandier, *Plasma Sources Sci. Technol.* **17**, 035016 (2008).
- ¹⁰Y. Cressault and A. Gleizes, *J. Phys. D: Appl. Phys.* **43**, 434006 (2010).
- ¹¹Y. Cressault, A. Gleizes, and G. Riquel, *J. Phys. D: Appl. Phys.* **45**, 265202 (2012).
- ¹²Ph. Teulet, J. J. Gonzalez, A. Mercado-Cabrera, Y. Cressault, and A. Gleizes, *J. Phys. D: Appl. Phys.* **42**, 175201 (2009).
- ¹³Ph. Teulet, J. J. Gonzalez, A. Mercado-Cabrera, Y. Cressault, and A. Gleizes, *J. Phys. D: Appl. Phys.* **42**, 185207 (2009).
- ¹⁴W. Wang, M. Rong, Y. Wu, J. W. Spencer, J. D. Yan, and D. Mei, *Phys. Plasmas* **19**, 083506 (2012).
- ¹⁵V. Colombo, E. Ghedini, and P. Sanibondi, *Plasma Sources Sci. Technol.* **20**, 035003 (2011).
- ¹⁶R. S. Devoto, *Phys. Fluids* **10**, 2105 (1967).
- ¹⁷V. Rat, P. André, J. Aubreton, M. F. Elchinger, P. Fauchais, and A. Lefort, *Phys. Rev. E* **64**, 026409 (2001).
- ¹⁸V. Rat, J. Aubreton, M. F. Elchinger, P. Fauchais, and A. B. Murphy, *Phys. Rev. E* **66**, 056407 (2002).
- ¹⁹S. Ghorui, J. V. R. Heberlein, and E. Pfender, *Plasma Chem. Plasma Process.* **28**, 553–582 (2008).
- ²⁰M. Rong, L. Zhong, Y. Cressault, A. Gleizes, X. Wang, F. Chen, and H. Zheng, *J. Phys. D: Appl. Phys.* **47**, 495202 (2014).
- ²¹L. Zhong, A. Yang, X. Wang, D. Liu, Y. Wu, and M. Rong, *Phys. Plasmas* **21**, 053506 (2014).
- ²²M. I. Boulos, P. Fauchais, and E. Pfender, *Thermal Plasmas: Fundamentals and Applications* (Plenum Press, New York, 1994), Vol. 1, pp. 225–234.
- ²³A. V. Potapov, *High Temp.* **4**, 48 (1966).
- ²⁴M. C. M. van de Sanden, P. P. J. M. Schram, A. G. Peeters, J. A. M. Van der Mullen, and G. M. W. Kroesen, *Phys. Rev. A* **40**, 5273 (1989).
- ²⁵A. Gleizes, B. Chervy, and J. J. Gonzalez, *J. Phys. D: Appl. Phys.* **32**, 2060–2067 (1999).
- ²⁶V. Colombo, E. Ghedini, and P. Sanibondi, *J. Phys. D: Appl. Phys.* **42**, 055213 (2009).
- ²⁷A. Kramida, Yu. Ralchenko, J. Reader, and NIST ASD Team, *NIST Atomic Spectra Database (Version 5.3)* (National Institute of Standards and Technology, Gaithersburg, MD, 2015).
- ²⁸M. W. Chase and C. J. Davies, *NIST-JANAF Thermochemical Tables*, 4th ed. (American Institute of Physics for the National Institute of Standards and Technology, New York, 1998).
- ²⁹X. Wang, L. Zhong, Y. Cressault, A. Gleizes, and M. Rong, *J. Phys. D: Appl. Phys.* **47**, 495201 (2014).

- ³⁰L. Zhong, X. Wang, M. Rong, Y. Wu, and A. B. Murphy, *Phys. Plasmas* **21**, 103506 (2014).
- ³¹R. S. Devoto, *J. Plasma Phys.* **2**, 617–631 (1968).
- ³²P. André, W. Bussiere, and D. Rochette, *Plasma Chem. Plasma Process.* **27**, 381 (2007).
- ³³A. Laricchiuta, G. Colonna, D. Bruno, R. Celiberto, C. Gorse, F. Pirani, and M. Capitelli, *Chem. Phys. Lett.* **445**, 133 (2007).
- ³⁴M. Capitelli, D. Cappelletti, G. Colonna, C. Gorse, A. Laricchiuta, G. Liuti, S. Longo, and F. Pirani, *Chem. Phys.* **338**, 62 (2007).
- ³⁵A. B. Murphy, *Plasma Chem. Plasma Process.* **20**, 279–297 (2000).
- ³⁶A. B. Murphy, *Chem. Phys.* **398**, 64–72 (2012).
- ³⁷A. Aubreton and M.-F. Elchinger, *J. Phys. D: Appl. Phys.* **36**, 1798–1805 (2003).
- ³⁸F. B. M. Copeland and D. S. F. Crothers, *At. Data Nucl. Data Tables* **65**, 273–288 (1997).
- ³⁹C. Bonnefoi, “Contribution à l’étude des méthodes de résolution de l’équation de Boltzmann dans un plasma à deux températures: exemple le mélange argon-hydrogène,” Ph.D. thesis, University of Limoges, France, 1983.
- ⁴⁰A. B. Murphy and C. J. Arundelli, *Plasma Chem. Plasma Process.* **14**, 451–490 (1994).
- ⁴¹X. Chen and H.-P. Li, *Int. J. Heat Mass Transfer* **46**, 1443–1454 (2003).
- ⁴²J. N. Butler and R. S. Brokaw, *J. Chem. Phys.* **26**, 1636 (1957).
- ⁴³V. Rat, P. André, J. Aubreton, M. F. Elchinger, P. Fauchais, and D. Vacher, *J. Phys. D: Appl. Phys.* **35**, 981–991 (2002).
- ⁴⁴V. Colombo, E. Ghedini, and P. Sanibondi, *Prog. Nucl. Energy* **50**, 921–933 (2008).